A Numerical Case Study of the Effects of Latent Heating on a Developing Wave Cyclone

C. B. CHANG[1], D. J. PERKEY AND C. W. KREITZBERG

Drexel University, Philadelphia, PA 19104

(Manuscript received 12 October 1981, in final form 22 March 1982)

ABSTRACT

The effects of latent heating on the development of a wave cyclone are investigated using a multi-level primitive equation model to simulate the cyclone system with (wet) and without (dry) latent heating. While the dry simulation failed to properly predict either the formation of the closed circulation which developed throughout the depth of the troposphere or the pronounced northwest-to-southeast horizontal tilt of the upper-level trough shown by observations, the wet simulation successfully reproduced both these features.

The mechanisms for the generation of the regional-scale closed system are examined and the influence of latent heating on large-scale dynamics and energetics is discussed. Results indicate that latent heat release stabilized the troposphere and reduced the large-scale horizontal temperature gradient. Also, through the enhancement of ageostrophic flow, the addition of latent heat generated kinetic energy in both the lower and upper troposphere at the expense of the available potential energy.

1. Introduction

Most midlatitude or extratropical synoptic-scale systems rely on large-scale baroclinic instability for their continued existence. The motion in most developing systems is primarily maintained by so-called baroclinic processes which convert available potential energy into kinetic energy. Holton (1972, pp. 96–101) and Palmén and Newton (1969, pp. 315–331) discussed a developing baroclinic system for adiabatic conditions using an idealized model. Their discussions described a developing system as being characterized by a westward tilt (in the vertical) of the pressure trough and ridge. In the horizontal, there was a lag (westward phase shift) of the thermal trough (thickness trough) behind the pressure trough. Under these conditions, temperature advection intensified both the upper-level pressure trough and ridge, and in response, the cyclonic circulation strengthened such as to balance the enhanced pressure gradient via the Coriolis force. At the same time, the ascent of warm air to the east of the trough and the descent of cold air to the west produced a thermally direct circulation which provided a source of energy to compensate for frictional dissipation. The system started to decay when the lag between the thermal field and the pressure field disappeared.

The development and dissipation processes of synoptic-scale systems are actually much more complicated than those of the above idealized case. One of the major complications is latent heat release. The latent heating, although not generally responsible for the creation of large-scale baroclinicity, can provide an additional energy source for the intensification of the system. Palmén and Newton (1969) discussed the impact of latent heat from the "self-development" viewpoint and concluded that " 'self-development' can proceed further and the cyclone can achieve greater intensity than it could if precipitation were absent." Krishnamurti (1968) investigated a developing wave cyclone using the vertical velocity as the basis for his discussion. He determined that during that period of the storm with one to two inches per twelve hours of precipitation, the latent heat's contribution to the vertical velocity was comparable to the contribution of all other terms and tended to increase the ascent over the storm area. Examples of other researchers who have discussed the role of latent heat on cyclone and large-scale development include Aubert (1957), Danard (1964) Charney and Eliassen (1964), and Tracton (1973).

The purpose of this study is to investigate the impact of latent heating on large-scale circulations. For this purpose, two real-data numerical experiments were conducted on the 20 May 1977 SESAME '77 case (Kreitzberg, 1977). This case, as described by Kreitzberg, developed severe convection in Oklahoma during the period from 1200 GMT 20 May to 1200 GMT 21 May. In addition to the Oklahoma convection, heavy rains were observed throughout the period in Nebraska, Kansas, Texas and eastward into Missouri.

The two numerical experiments were 1) a 24 h

[1] Present affiliation: Department of Meteorology, University of Wisconsin, Madison 53706.

0022-4928/82/071555-16$08.00

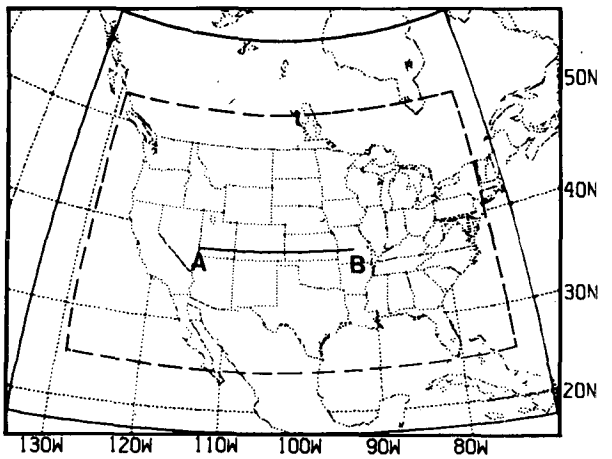

FIG. 1. Model integration domain (outlined by the heavy solid latitude-longitude lines) with location of cross section AB discussed in Figs. 12–14. The heavy dashed line incloses the averaging area discussed with Fig. 11.

fine-mesh (~140 km) simulation without latent heating, i.e., a "dry" simulation and 2) a 24 h fine-mesh simulation with latent heating, a "wet" simulation. These experiments were designed to test the hypothesis that without latent heating the intensity of wind circulation, as well as the pressure gradient, of the synoptic system becomes considerably weaker than the circulation of the wet system.

A brief description of the model and analysis procedures is contained in Section 2 while in Section 3 we discuss the observed storm system of 20–21 May 1977. The results of the two simulations are presented in Section 4 and in Section 5 we discuss diagnostic studies of the interaction between the dynamics and the latent heating by analyzing the differences in the forecasts between the wet and dry simulations and their energetics.

2. Analysis and prediction techniques

The numerical simulations for these experiments employed the Drexel/NCAR Limited Area Mesoscale Prediction System (LAMPS). This system contains a moist hydrostatic primitive equation model which includes non-convective condensation processes due to large-scale ascent (Perkey, 1976) as well as a one-dimensional sequential plume model for parameterizing the moist convective processes (Kreitzberg and Perkey, 1976).

The model used a 1.60° longitude by 1.25° latitude grid in the horizontal and terrain following coordinates in the vertical. The vertical transformation function is given by $h = (z - E)H/(H - E)$ where z and E are the height above mean-sea-level and terrain elevation, respectively. The height H was selected to be 5.25 km; above this height, h is equal to z. For the experiments discussed in this paper, the following 15 model levels were employed: 0.0, 0.025, 0.375, 0.750, 1.25, 2.0, 3.0, 4.5, 6.0, 7.5, 9.0, 10.5, 12.0, 14.0 and 16.0 km.

The model domain is shown in Fig. 1. Porous sponge boundary conditions (Perkey and Kreitzberg, 1976) were applied at the lateral boundaries. The initial state for the two runs was obtained from objective analysis of rawinsonde observations as designed by Bleck (1975). A more detailed description of the model characteristics and analysis procedures can be found in papers by Perkey (1976) and Chang *et al.* (1981).

3. The observed system

Fig. 2 shows the 700, 500 and 300 mb constant pressure maps as analyzed by the National Meteorological Center (NMC) at 1200 GMT 20 May 1977 (i.e., traces of NMC facsimile maps). At 700 mb, the major synoptic features were a low over the Rocky Mountain region and a high over the eastern United States. A region of very dry air existed from central Texas west to California with a pronounced dry band oriented in the north–south direction from Texas to North Dakota over the Plains states. This dry band separated the cold but moist air to the west (over Idaho, Utah and Wyoming) from a narrow zone of warm, very moist air to the east over Iowa, Missouri and Arkansas. Note that there was marked cross-contour flow along the eastern edge of the dry band. The confluence of relatively strong southerly current within the zone of large height gradient and the cross-contour flow was associated with an outbreak of convective activity as shown in Fig. 4a. The thermal trough over the western states lagged behind the height trough by ~500 km. The wind circulation indicated cold advection behind the low system with warm advection ahead of the low.

At 500 mb, a cold, moist trough existed over the western states while a warm, dry ridge was present over the eastern states (moisture not shown). The isotherms, which were almost parallel to the height contours, suggested weak thermal advection. The temperature gradient was large in the vicinity of the trough and considerably weaker near the ridge. A jet streak (not shown) extended from southern California to the Texas Panhandle with a maximum speed of 70 m s^{-1} located in northern Mexico where a large low-level temperature gradient was observed. The axes of the height contours appeared to tilt eastward with latitude. Similar to that at 700 mb, there was a marked dry tongue over the Great Plains states with confluence of flow along its eastern edge.

At 300 mb, the pattern and the orientation of the height contours was similar to that at 500 mb. Again there was a cold trough and warm ridge with isotherms almost parallel to the height contours.

Between 700 and 500 mb, there was a notable tilt

of the height contours toward the cold air in the lower troposphere while the axes of the thermal trough had the opposite tilt. As discussed in the Introduction, this phase relationship between the height and thermal troughs in the lower atmosphere is favorable for the motion field to convert available potential energy into kinetic energy and develop a low-level closed circulation. In the upper levels, the axes of the height trough and thermal trough were almost vertical with height. In general, the upper-level structure did not represent a baroclinically active situation. The horizontal trough orientation suggested weak transport of westerly momentum out of the strong westerly flow in the south.

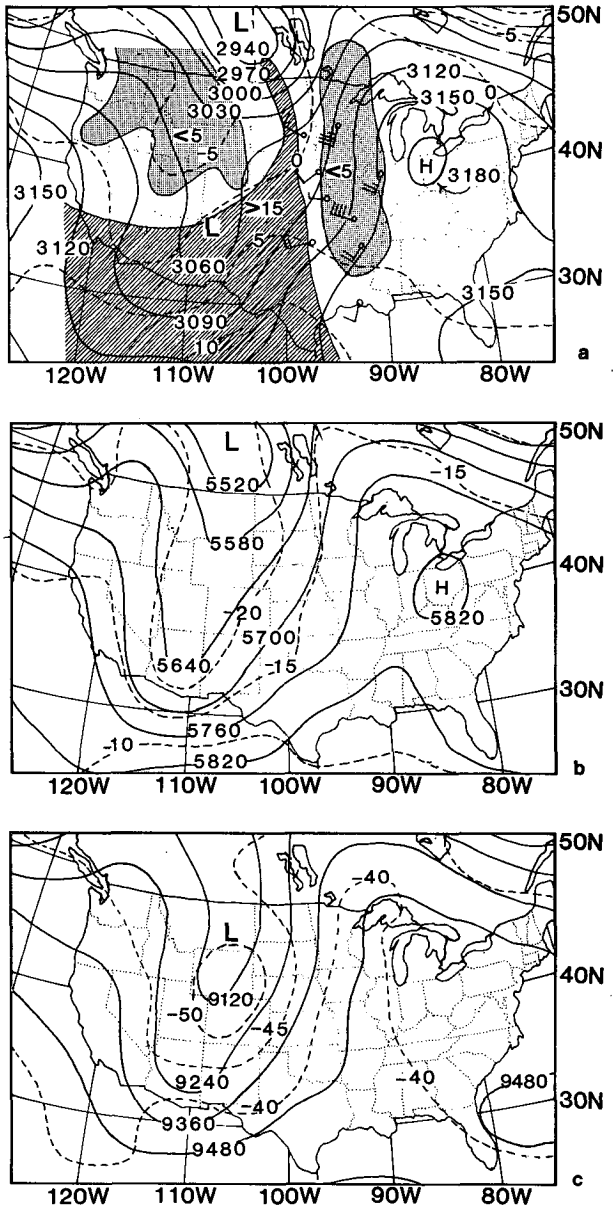

FIG. 2. NMC height (solid lines) and temperature (dashed lines) analyses at 1200 GMT 20 May 1977 for (a) 700 mb, (b) 500 mb and (c) 300 mb. The height contour interval is 30, 60 and 120 m, respectively. The temperature interval is 5°C in all figures. Part (a) includes selected wind observations and the stippling denotes dewpoint depressions of greater than 15°C and less than 5°C as noted.

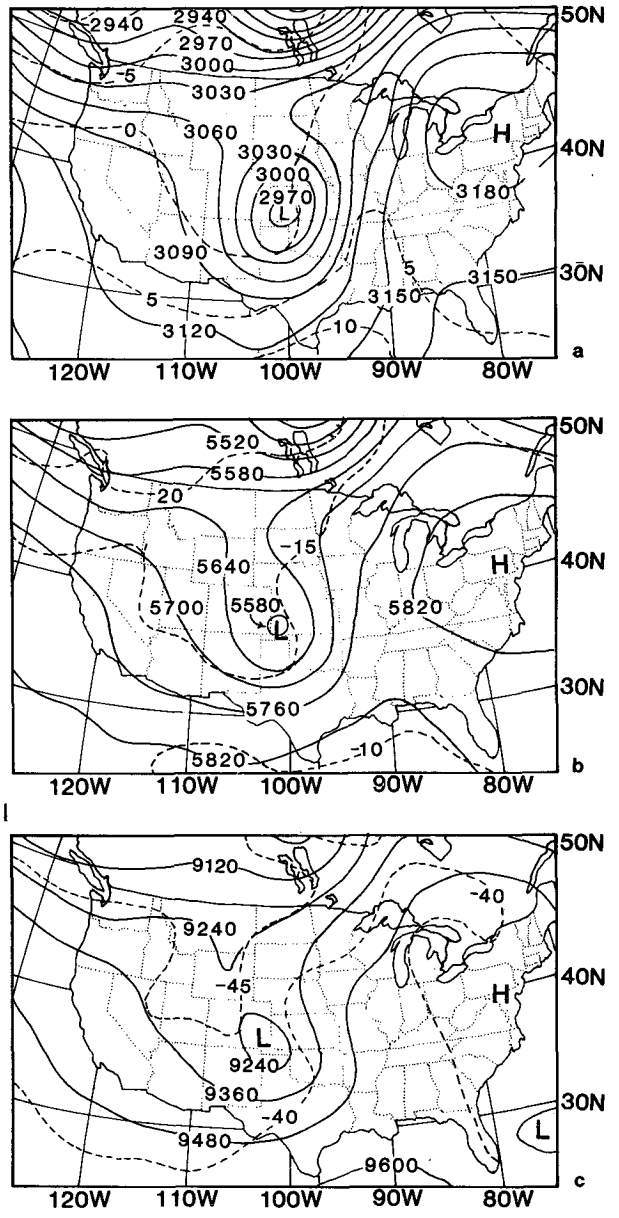

FIG. 3. As in Fig. 2 but for 1200 GMT 21 May 1977. Wind and dewpoint depression observations are not included.

Fig. 3 shows the 700, 500 and 300 mb analyses provided by NMC for 1200 GMT 21 May 1977. The 24 h changes in the 700 mb height field are most notable. A well defined closed system with its low center located in western Kansas has developed. A dramatic drop of over 100 m in height at the low center has occurred while the changes in the high in the east were considerably less. Both the low and

high centers propagated eastward ~800 km in 24 h; however, note that the 3150 m contour remained in almost the same location during this period. Thus, in addition to deepening, the low has moved so as to increase the height gradient to its east more rapidly than to its west. This enhanced eastern gradient resulted in an intense circulation which advected warm air from the south as cold air flowed down from the north; the baroclinic zone then rotated around the low to a location over Texas and Oklahoma in response to the advection as moderated by the vertical motion. The relatively warm low has become a cold-core system as the thermal trough moved closer to the low center. This temperature-height phase relationship is quite often observed in a deep, mature, synoptic-scale disturbance.

The most notable 24 h changes in the 500 mb height field were, again, the development of a closed low from an open trough and the large increase in height gradient on the eastern side of the low system as it moved eastward. Also, the axis of the trough has changed its horizontal orientation from eastward to westward with increasing latitude. Although the temperature has increased in the low center, it has retained its cold-core structure. Note that the temperature gradient located in the base of the trough in Fig. 2b has weakened during the 24 h period by Fig. 3b. A well-defined jet stream (not shown) was located along the eastern edge of the large height gradient region over the Great Plains states.

At 300 mb, the major changes were very similar to those at 500 mb. A low system possessing an axis tilted westward with increasing latitude and a closed circulation was located at the border between Colorado and Kansas. A general reduction in horizontal temperature gradient was noted. At both the 500 and 300 mb levels, because of increased temperatures over the region of lower height, it appeared that the height trough tended to shift slightly ahead of the thermal trough. This is most clear at 300 mb where the cold-core structure started to disappear. Correspondingly, the 300 mb low was slightly to the west of the 500 mb low. The overall 24 h changes show that the low-level system has continued to intensify and has reached a mature state with a deeper cold low and a strong closed circulation at all levels. In the upper troposphere, the horizontal temperature gradient has been greatly reduced and the trough orientation has been changed from NE/SW to NW/SE.

Fig. 4 shows the radar summary charts for 1135 GMT 20 May, 2335 GMT 20 May and 1135 GMT 21 May 1977. Initially the major convective activity occurred along a north-south oriented band across the central United States. This band was to the east of the low-level trough and dissipated during the following 6 h as it moved eastward losing its large-scale support. By 2000 GMT (radar map not shown) convection associated with the low-level trough had developed. At 2335 GMT 20 May (Fig. 4b), a large area of convection over northern Texas, western Oklahoma, western Kansas and eastern Colorado was present. This widespread convection, which lasted for almost another 12 h, was closely related to the dynamic system. It was tied to the eastern and northeastern edges of the low-level cyclone and thus moved eastward with the cyclone. At 0600 GMT (not shown), a squall line appeared over central Texas. This squall system moved across eastern Texas and northward. By 1135 GMT 21 May (Fig. 4c), the convective area associated with the low-level system had almost disappeared while a north-south band across Nebraska, Kansas, Arkansas and Louisiana dominated the radar map. Considering the large horizontal dimensions and rather long duration of the convective activity associated with the cyclone, it is expected that latent heating might have had a significant impact on the dynamics and the energetics of the cyclone.

4. Results of the fine-mesh simulations

a. The 24 h dry run

Fig. 5 shows the 24 h 700, 500 and 300 mb dry simulation results. The model successfully simulated the formation of a closed system at 700 mb but did not capture the closing of the 500 and 300 mb systems. The 24 h change in the orientation with latitude of the upper-level trough from a positive north–south tilt to a negative tilt also was predicted. However, the predicted tilt in the 300 mb trough was much less than that observed. As compared with the NMC analyses (Fig. 3), the phase speed of the model system was slower and its intensity considerably weaker; for example, the height contour near the 700 mb cyclone center was 100 m higher than observed and the location of the center was misplaced by ~300 km (about two grid points) to the southwest. Also, the height gradient was weaker. Note that the predicted thermal structure associated with the low system showed warmer temperatures and weaker gradients at 700 mb, and colder temperatures and stronger gradients at 500 and 300 mb than those observed. Thus, the model has preserved the relatively warm low at the 700 mb level and the initial cold-core structure at upper levels. It is interesting to note that neither the NMC barotropic model nor the NMC limited-area fine-mesh (LFM) model predicted the development of the closed 500 mb system. Both NMC 24 h forecasts appeared to develop the system similar to that predicted by this dry simulation even though precipitation was predicted by the LFM in the general area of the system.

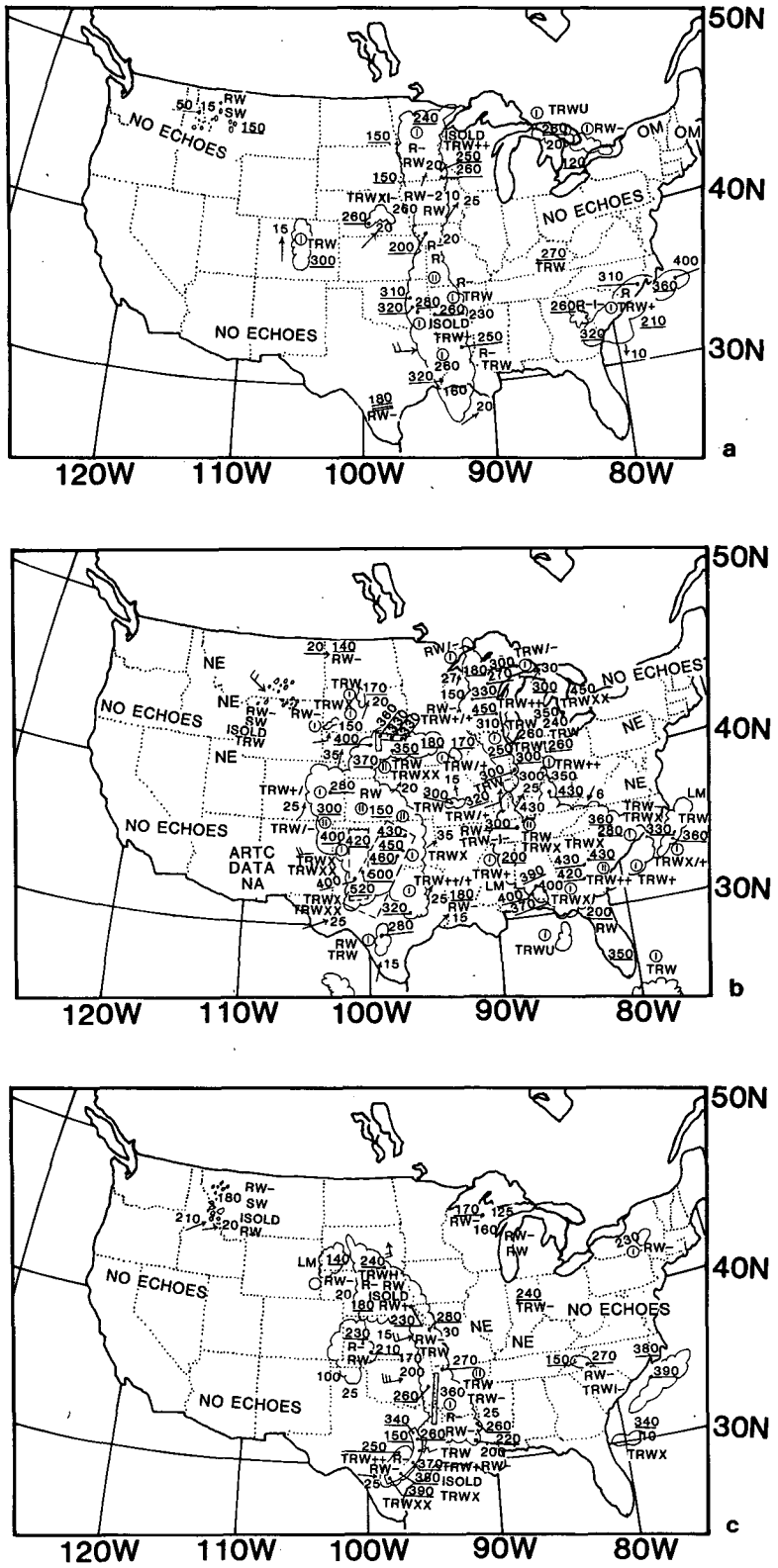

FIG. 4. Radar summary charts for (a) 1135 GMT 20 May (cf. Fig. 2), (b) 2335 GMT 20 May and (c) 1135 21 May 1977 (cf. Fig. 3).

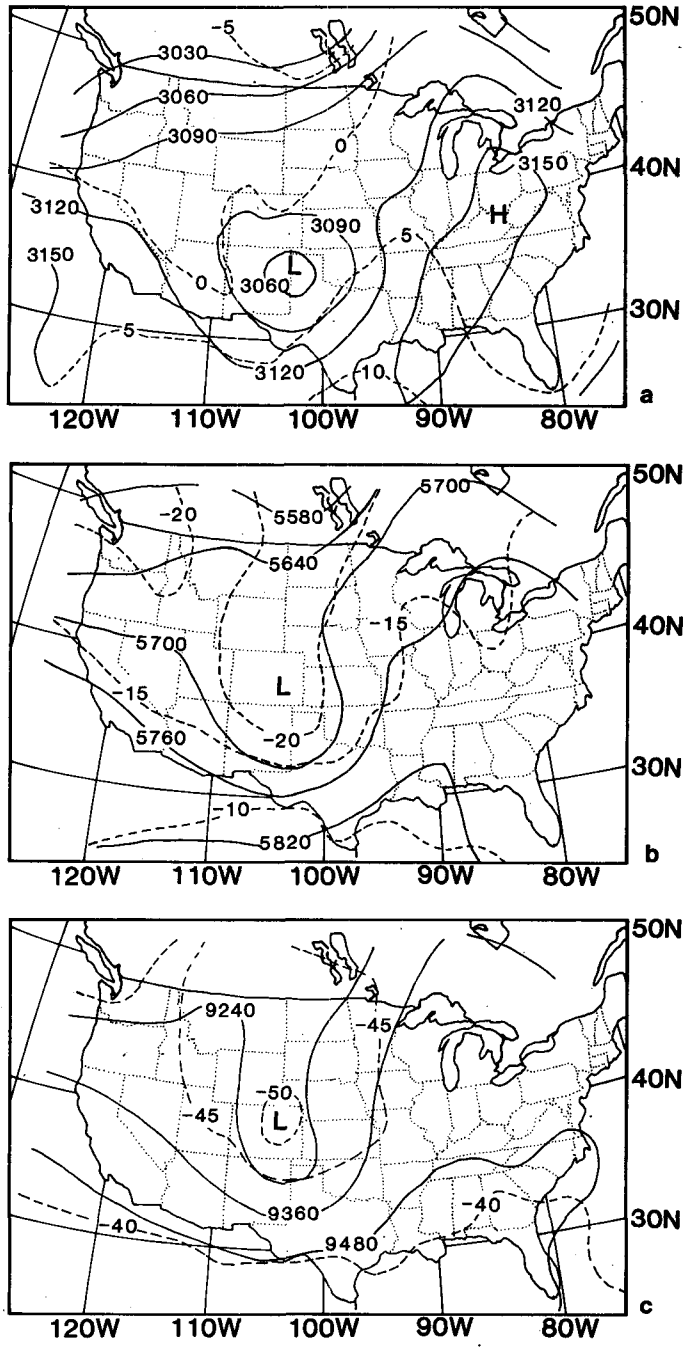

FIG. 5. Dry model simulated height and temperature at 1200 GMT 21 May 1977 for (a) 700 mb, (b) 500 mb and (c) 300 mb. Compare Fig. 3.

Fig. 6 presents the 24 h predicted 500 mb vertical motion and 300 mb relative vorticity fields. The 300 mb cyclonic vorticity associated with the trough was concentrated over the Texas panhandle. The relatively large region of 500 mb ascent in Texas, Oklahoma and Kansas was located directly under the area of maximum 300 mb vorticity gradient. Such a distribution, in conjunction with the weak temperature advection as indicated by the 700 and 500 mb maps (Figs. 5a and 5b) suggested that differential vorticity advection may be primarily responsible for generating the rising motion. The smaller region of descent over New Mexico appeared to be related to weak cold advection and the downslope motion of the cold

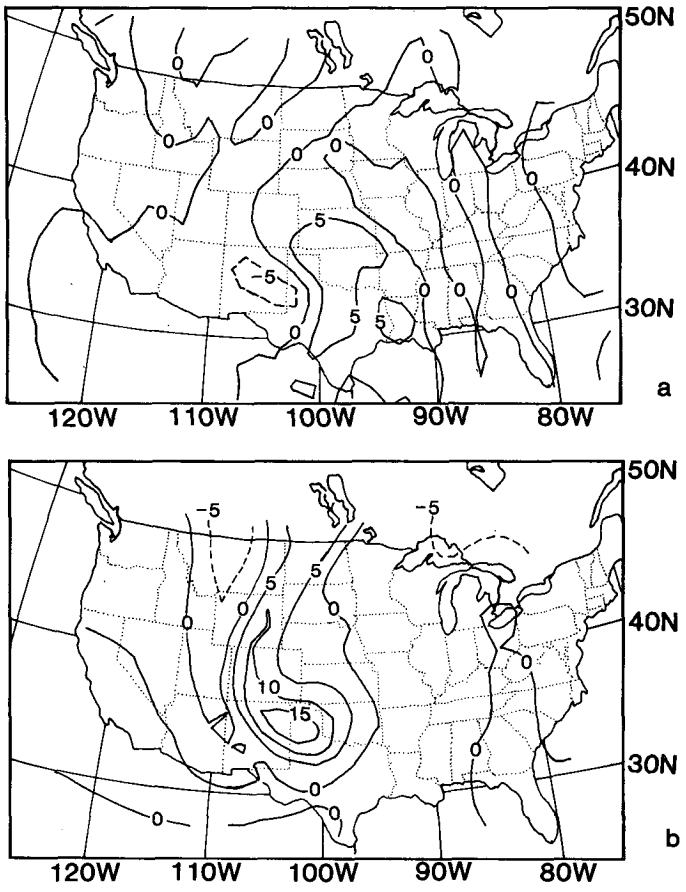

FIG. 6. Dry model simulated (a) 500 mb vertical velocity (cm s^{-1}) and (b) 300 mb relative vorticity (10^{-5} s^{-1}). The vertical velocity and vorticity intervals are 5. The dashed lines denote negative values.

air. The vertical motion patterns at 300 and 700 mb (not shown) were in phase with those at 500 mb.

b. The 24 h wet forecast

Fig. 7 shows the 24 h 700, 500 and 300 mb wet forecast maps. The wet model, as contrasted to the dry model, has successfully predicted the formation of closed systems at all levels. This is in better agreement with the NMC analyses. The location of the low center, the orientation of the trough, and the major features of the thermal pattern were in good agreement with observations; however, there were some disagreements. In general the model's central pressures were 30 m too high and were located slightly (less than one grid point) to the west of the observed system. A possibly more critical difference occurred at 300 mb where the model did not maintain the intensity of the high in the east and thus failed to catch the rather large height gradient over eastern Kansas and Nebraska (Fig. 3c). The corresponding weaker circulation, which did not bring enough warm air northward, may be responsible for the failure of the model to produce the pronounced temperature gradient observed to the north of the closed low. However, in comparison with the dry run, the wet forecast system phase speed and intensity were superior. Also, the temperature pattern in the vicinity of the trough was better represented.

Fig. 8 shows the predicted 500 mb vertical velocity and 300 mb relative vorticity fields. The basic structure of the vorticity distribution was similar to that of the dry run, but the magnitude was larger and the gradient was considerably stronger. One notable difference in the 300 mb vorticity between the wet and dry runs was the formation of a band of negative relative vorticity over north-central Colorado, eastern Wyoming, western South Dakota and southeastern North Dakota. These negative values and the larger positive values over northern Texas as well as the stronger horizontal gradient over Kansas and Oklahoma in the wet run were consistent with the curvature and shear of the wind circulation suggested in the height difference maps (Fig. 11, discussed later). The large concentration of vorticity over New Mexico and Texas showed an east–west orientation

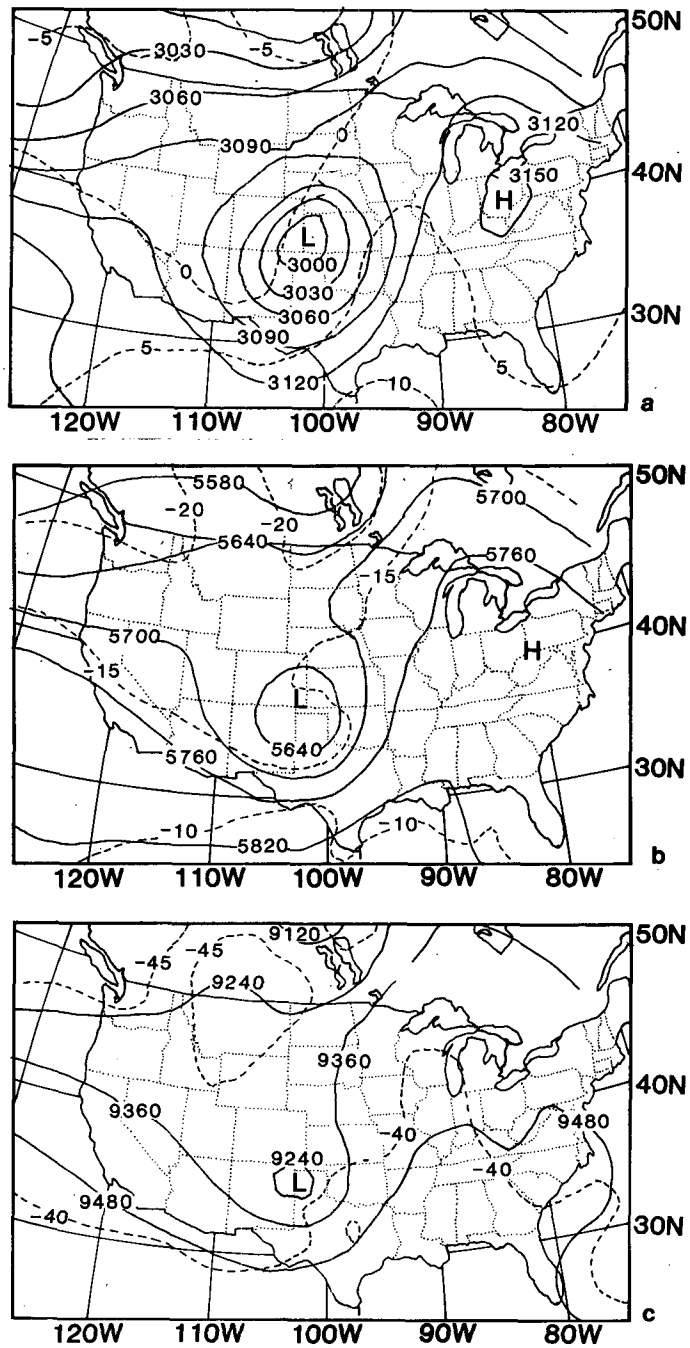

FIG. 7. As in Fig. 5 except for the wet model simulation. Compare Figs. 3 and 5.

indicating sizeable northward vorticity advection over the center of the 700 mb cyclone into Kansas and Nebraska.

The wet 500 mb vertical motion showed much larger ascent along the eastern and northern edges of the low system than did the case without latent heating. This agrees with the diagnostic results obtained by Krishnamurti (1968) mentioned in the Introduction. The maximum value (over 20 cm s^{-1} as compared to less than 10 cm s^{-1} for the dry case) was correlated with the maximum 700 mb height gradient over northeastern Colorado and northwestern Kansas (Figs. 3a and 5a). This tight gradient and its associated ascent was directly related to the latent heat release (see Fig. 10a). Throughout the troposphere, the ascent was correlated with the warm

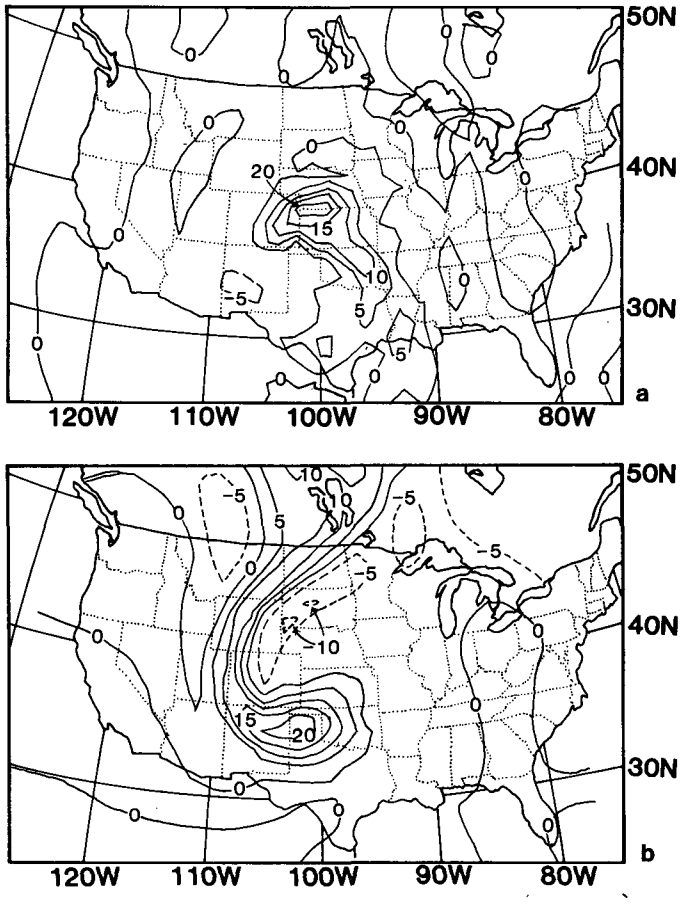

FIG. 8. As in Fig. 6 except for the wet model simulation. Compare Fig. 6.

air and the subsidence with the cool air. However, in spite of its stronger direct circulation, the wet case 700 mb temperature gradient near the closed system remained stronger than did the corresponding dry case gradient. In the upper levels, the situation was reversed; the dry case showed a larger thermal gradient associated with the trough than did the wet case. In comparison with the wet run, the latent heating tended to destroy the thermal contrast in the upper troposphere, while at the same time the dynamic response to the heating acted to convert the available potential energy generated by the heating into kinetic energy in support of the increasing wind circulation (more discussion follows in Section 5c).

Fig. 9 depicts the predicted convective precipitation rate [mm 10^{-4} s^{-1} $\approx$ mm $(3\ h)^{-1}$]. The initial north–south convective band (prediction not shown) over the central United States was not captured by the model; only the part of the band over Texas was predicted. However, recall that from Section 3 this band dissipated during the next 6 h as it moved eastward and lost its large-scale support. At 0000 GMT 21 May (Fig. 9a), the primary convective activity associated with the cyclone verified well with the radar summary chart (Fig. 4b) only missing a narrow east–west oriented band over Nebraska. The model failed to reproduce the secondary convective regions over Wisconsin and Illinois and only hinted at the convection over the southeastern United States. At 1200 GMT 21 May (Fig. 9b), the agreement was not as good. It appeared that at this time the convection due to the synoptic disturbance weakened as observed (Fig. 4c) but the convection which developed along the Kansas-Missouri, Oklahoma-Arkansas borders and over east Texas was east of that predicted by the model.

Fig. 10 shows the accumulated total precipitation (combination of stable and convective precipitation) for the 24 h forecast period and the corresponding observed values from the precipitation network. A maximum of over 60 mm was predicted in western Kansas. The area of large precipitation in Nebraska, Colorado and Kansas compared quite well with the observations albeit the predicted maximum was displaced slightly to the southwest. The secondary precipitation maximum over southeastern Missouri along

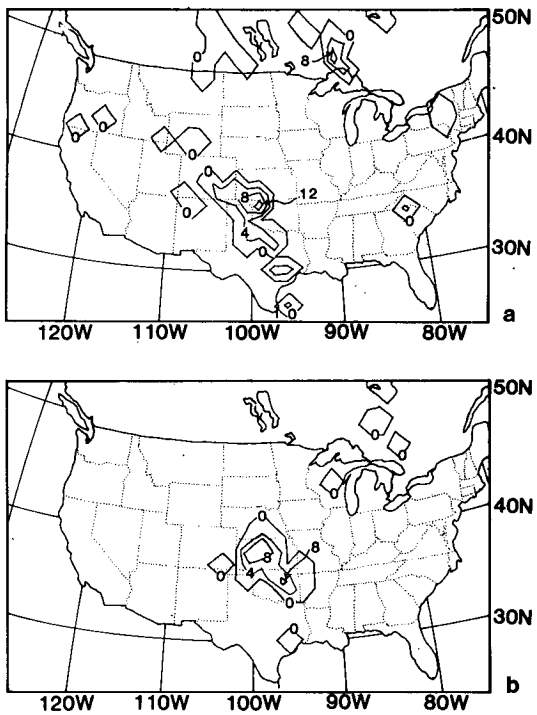

FIG. 9. Predicted convective precipitation rate [mm 10^{-4} s^{-1} or ~ mm $(3\ h)^{-1}$] at (a) 0000 GMT (cf. Fig. 4b) and (b) 1200 GMT 21 May 1977 (cf. Fig. 4c). The contour interval is 4.

with the substantial rain in southeastern Texas and Louisiana were missed. Notice that the Illinois and Wisconsin convection that the model missed did not produce significant rainfall and that the observed rainfall north of Lake Superior was predicted.

In summary, although the model did not completely reproduce all of the observed precipitation features, the simulation did capture the primary precipitation features associated with the cyclone development and thus can yield valuable insight into the impact of latent heat on the cyclone system especially during its intensification stage.

5. Results of the diagnostic studies

a. Dry and wet simulation differences

In order to better understand the significance of the latent heat release on this developing cyclone, this section depicts the results using difference maps. These maps were constructed by subtracting the predicted dry values from the corresponding predicted wet values. Fig. 11 presents the 24 h forecast height, temperature and vector wind differences on the 700, 500 and 300 mb pressure surfaces, respectively. Note that, as expected, the maximum differences occurred over the regions of intense precipitation (Fig. 10a). The major patterns were a (relative) cold low at 700 mb, a warm low at 500 mb, and a warm high at 300 mb. Throughout the troposphere there was a net increase in the area-mean (calculated over the region inclosed by the heavy dashed line in Fig. 1) 24 h predicted temperature due to the latent heat release. This temperature increase was largest at 300 mb (0.85°C) decreasing in magnitude downward to 700 mb (0.03°C). The height difference field indicated an average increase in the 700–500 mb thickness of 5 m and an increase in 500–300 mb thickness of 13 m. Comparing the vertical velocity fields between the wet (Fig. 8a) and dry simulations (Fig. 6a), the wet case produced much larger upward motion in the area of positive temperature difference at 500 mb. This indicates that the latent heating exceeded the adiabatic cooling and thus the air column was forced to expand. Consequently, relative high- and low-pressure areas were generated in the upper and lower troposphere, respectively.

At 300 mb, the generation of a high to the north acted to fill the northern portion of the trough and the generation of lower heights to the south tended to deepen the southern portion of the trough. As a result, this led to the formation of a cut-off low as shown in the wet run. The corresponding change in wind circulation at 300 mb enhanced the north–south temperature advection. These processes, in conjunction with latent heating, appeared to be responsible for the distribution of positive temperature difference over a rather wide region. At 500 mb, the largest temperature differences were confined to the areas of large precipitation indicating that latent heating and adiabatic cooling were the main factors in determining its pattern, i.e., the effects of the latent heat were only partially advected out of the region. Note that, at both 500 and 300 mb, the increase in temperature due to the inclusion of condensation processes occurred largely in the colder air. Thus, the upper-level baroclinicity was reduced. At 700 mb, the change in temperature was related more to the change in the height field and the associated wind field than to the adiabatic and diabatic processes. As shown later, the dry static energy ($c_pT + gz$) differences indicated that the effects of condensation worked to stabilize the lower troposphere and destabilize the upper troposphere in the region of the precipitation.

As was expected, the upper-level high in the geopotential difference field and its pronounced gradient were located over the low-level relative warm air and its strong gradient, respectively. The area of negative geopotential difference was tilted southward away from the positive differences in temperature. This vertical distribution is in agreement with the thermal wind relationship.

In response to the enhancement of the height gradient, the winds increased their cyclonic circulation at 700 and 500 mb and their anticyclonic circulation at 300 mb. As evidenced by the increased vertical motion, the wet case low-level winds had a stronger

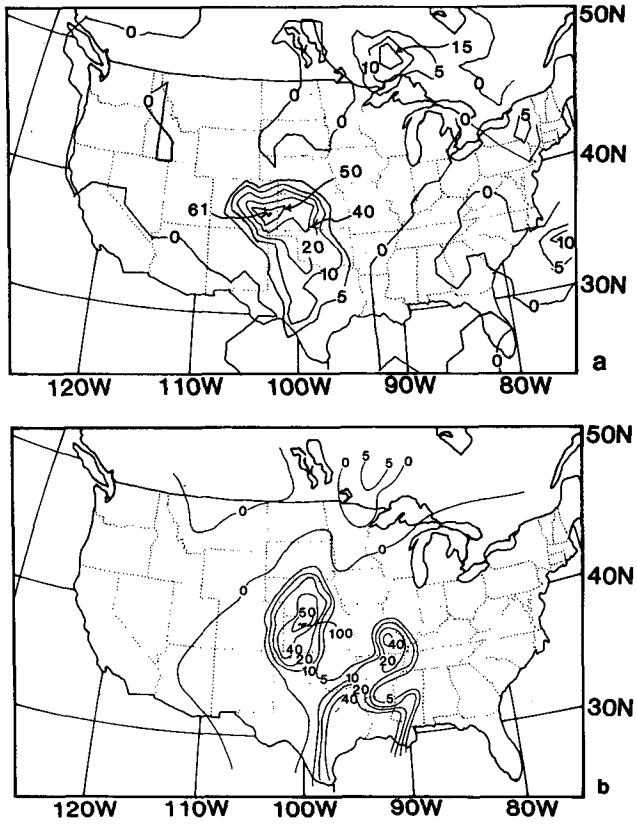

FIG. 10. 24 h accumulated precipitation (mm) ending at 1200 GMT 21 May 1977: (a) predicted and (b) observed.

cross-contour component than did those of the dry case. The maximum wind difference was 21 m s^{-1} at 700 mb, 14 m s^{-1} at 500 mb and 35 m s^{-1} at 300 mb. At all three levels this maximum occurred over the northwest quadrant relative to the precipitation field (Fig. 10a).

b. Vertical cross sections

Figs. 12 and 13 show the 24 h vertical cross sections of the simulated tangential, normal and vertical wind components and the relative vorticity along the line AB (see Fig. 1) for the dry and wet simulations, respectively. The line AB was chosen to cut through the area of maximum precipitation which occurred several hundred kilometers north of the 300 mb cut-off low as predicted in the wet simulation. The dashed lines represent the contours of dry static energy. Fig. 14 shows the corresponding cross section of heating rates due to convective and non-convective condensation. The convective precipitation was defined as that precipitation predicted by the convective parameterization scheme while the non-convective or stable precipitation was that precipitation resolved by the model grid and was calculated by the primitive equations for rainwater fallout (see Perkey, 1976). The dashed contours in Fig. 14 are moist static energy ($c_pT + gz + Lq$), where L is latent heat of condensation and q the specific humidity. The location of the center of the disturbance may be identified by the zero contour line in the normal component of the wind (at the ground, ~1200 km along the abscissa).

The main features and differences between the simulations in the vicinity of disturbance center are described below:

1) The distribution of dry static energy (dashed lines) showed a less stable and more baroclinic atmosphere in the dry case (Fig. 12a) than in the wet case (Fig. 13a) below 7 km, and a more stable atmosphere above. These differences were attributed to latent heating which effectively warmed the cold air in the middle-upper troposphere in the wet case.

2) As shown in the difference maps, latent heating caused a significant change in the height patterns. The corresponding change in wind circulation was evident in the cross section of u and v; for example, in the wet forecast a region of upper-level strong easterlies (Fig. 13a, 1000 km along the abscissa and 10 km on the ordinate) and a surface northerly jet (Fig. 13b; 800 km, 3 km) were generated along with

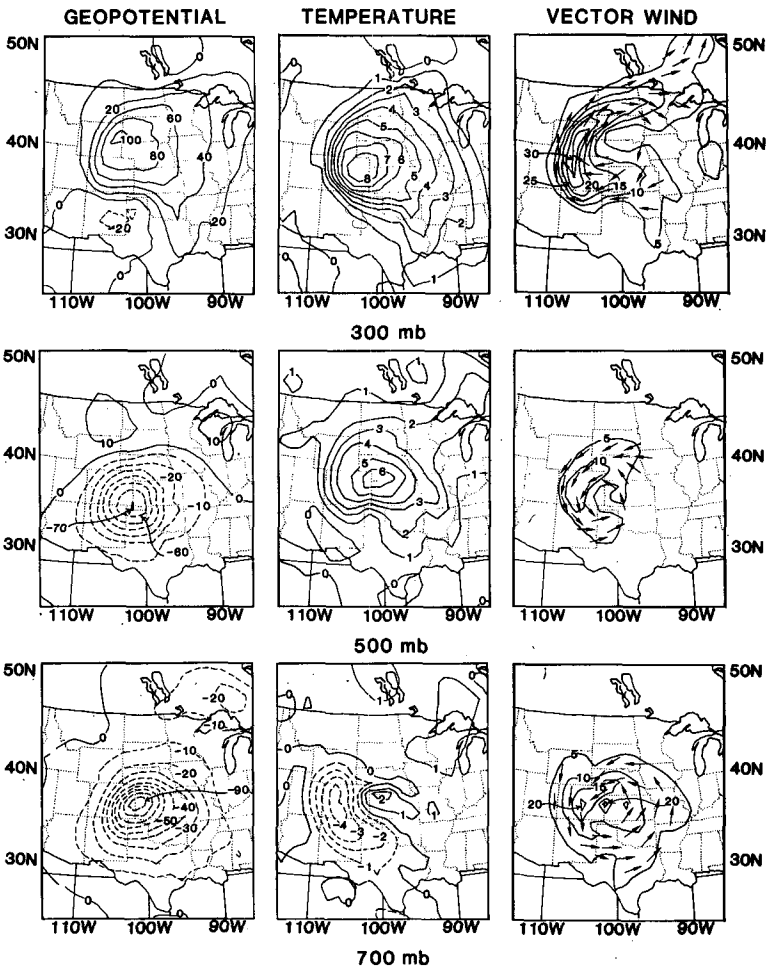

FIG. 11. Simulated 700, 500 and 300 mb wet minus dry geopotential height, temperature and vector wind difference fields at 1200 GMT 21 May 1977. The height interval is 10 m on both the 700 and 500 mb levels and 20 m on the 300 mb level, the temperature interval is 1°C for all three levels, and the isotach interval is 5 m s^{-1}. The dashed contours denote negative differences.

a weakening of the wind shear on the western side of the upper-level jet (Fig. 13b; 1000 km, 10 km). The large differences in the horizontal and vertical wind shear associated with these jets between the two runs suggested a change in energy source for maintaining the motion fields. Note that the decrease in higher level wind speed was correlated with the decrease in lower-level thermal contrast.

3) The vertical motion fields showed similarities in their general patterns. In the wet case, however, much larger upward motions were directly related to the latent heating. In the dry case, the upward motion occurring in the regions of rather weak stability (Fig. 12c; 1400 km, 7 km) appeared to be forced by the differential advection of vorticity. Away from the areas of latent heating there was little difference in magnitude between the two cases (0–500 and 1600–2000 km along the abscissa).

4) The vertical distribution of relative vorticity in the dry case showed weak cyclonic vorticity below 7 km at 1200 km (Fig. 12d), while in the wet case (Fig. 13d) a large concentration of cyclonic vorticity within a deep, narrow column below 6 km at 1100 km was apparent. This vorticity maximum was correlated with the cyclonic shear of the normal wind component. Also, there was a decrease in vorticity at upper levels (750 km, 8 km) due to the inclusion of latent heat; thereby, indicating the development of a relative high aloft.

Based upon the preceding discussion, the effects of latent heating on the development of the wave cyclone in this case study are summarized below. Latent heat release caused strong warming in the layers between 3 and 8 km with a maximum on the order of 80°C day^{-1} occurring near 7 km (Fig. 14). Note that the convective forced warming (Fig. 14a) dominated the stable heating (Fig. 14b) in this case. This heating generated low-level convergence and upper-level divergence through the hydrostatic pres-

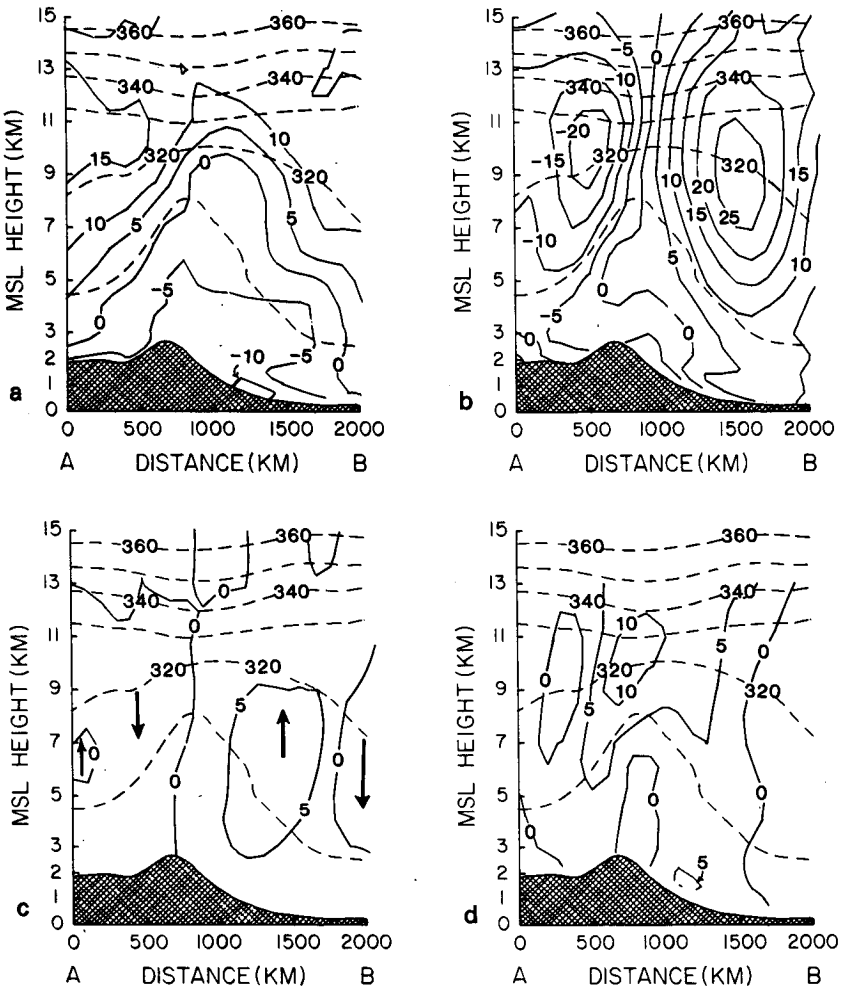

FIG. 12. Dry model simulated vertical cross sections along line AB (shown in Fig. 1) at 1200 GMT 21 May 1977: (a) horizontal wind component tangent to the cross section (m s^{-1}), (b) horizontal wind component normal to the cross section (m s^{-1}), (c) vertical velocity (cm s^{-1}) and (d) relative vorticity (10^{-5} s^{-1}). The contour intervals are 5 for all quantities. The dashed lines are contours of dry static energy (10^3 m^2 s^{-2}). The dry static energy interval is 10.

sure adjustment (Fig. 11). The associated vertical velocity and adiabatic cooling tended to offset the latent heating. Because the warming exceeded the adiabatic cooling, a net increase in temperature in the middle layers was observed (Fig. 11). The net heating and expansion of the air column resulted in height rises to the north and height falls in the south at 300 mb, and height falls at and below 500 mb. These processes led to the formation of a cut-off low throughout the troposphere enhancing the NW/SE tilt of the trough in the upper troposphere. Meanwhile, because heating effectively warmed the middle troposphere, the lower atmosphere became more stable and the horizontal temperature gradient associated with the large-scale motion was reduced. In response to these changes in the height and temperature fields, a secondary circulation with a scale <1000 km was generated within the large-scale pattern over the regions of intense precipitation. In the upper troposphere, this circulation tended to counter the large-scale flow and thus slowed down the jet around the trough. In the lower troposphere, this circulation strengthened the cyclonic flow through the development of a low-level jet. Thus latent heating changed the configuration of the jet from a large-scale pattern with pronounced vertical shear into a small-scale feature with marked horizontal shear. This process of transferring momentum from a larger scale to a smaller scale feature was carried out primarily by the adjustment of the velocity field to the mass field.

The latent heating also affected the horizontal orientation of the upper-level trough. The orientation of the trough is closely related to the north–south exchange of momentum, the distribution of which influences the propagation speed and direction of the

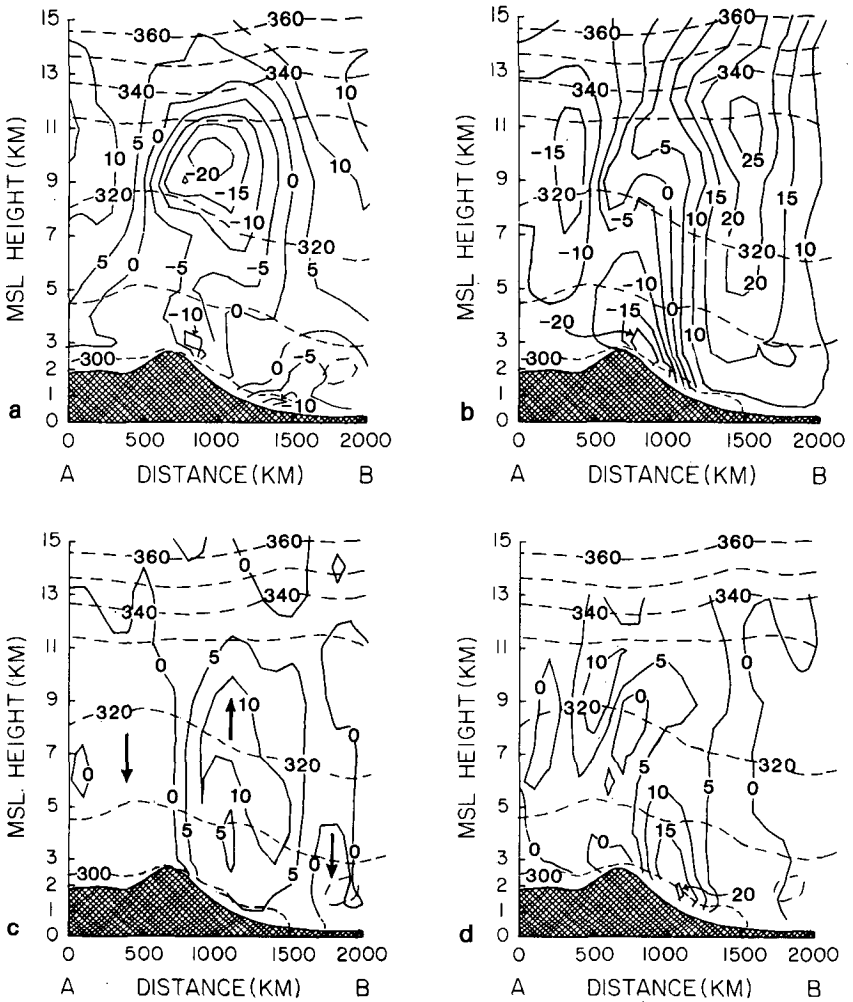

FIG. 13. As in Fig. 12 except for the wet model simulation.

low-level system. This may be one of the reasons why there was a few hundred kilometers difference in the location of 700 mb low center between the cases (Figs. 5a and 7a).

c. *Dry and wet simulation energetics*

Two basic components of energy in the atmosphere were computed: available potential energy (APE) and kinetic energy (KE). The expressions for APE and KE, according to Lorenz's (1967) approximations, are

$$\mathrm{APE} = \frac{1}{g}\int \left\{ \frac{\frac{c_p}{2}\iint \frac{\Gamma_d}{\Gamma_d - [\Gamma]}\frac{[T''^2]}{[T]}\,dxdy}{\iint dxdy} \right\} dp,$$

$$\mathrm{KE} = \frac{1}{g}\int \left\{ \frac{\frac{1}{2}\iint (u^2 + v^2)dxdy}{\iint dxdy} \right\} dp,$$

where Γ is the lapse rate of temperature and Γ_d the dry adiabatic lapse rate. The brackets denote an average over the entire isobaric surface within the averaging domain (see Fig. 1) and the double prime denotes the departure from the average; u and v are the west-to-east and the south-to-north wind components, respectively.

Tables 1 and 2 show the computed APE and KE every 6 h for the dry and wet simulations, respectively. KE was calculated for the upper atmosphere (150–500 mb), the lower atmosphere (500–850 mb), and the total depth of the atmosphere (850–150 mb), while the APE was calculated for the total depth only. They showed that in both cases the modeled atmosphere's domain-averaged KE and APE decreased with time. These parameters should not be expected to be constant since the boundaries allow information to both enter and exit the domain; however, the same information is entering both the dry and wet simulations. A complete energy budget would be required to determine whether the model was conserving energy or not. Baumhefner and Dow-

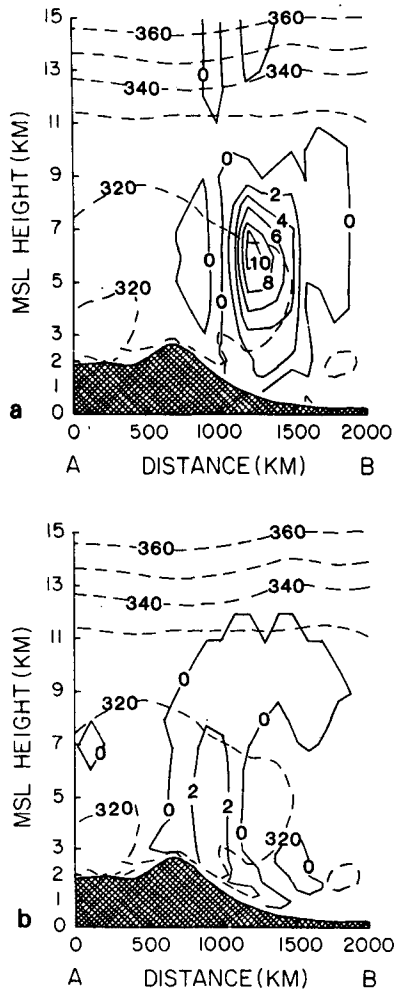

FIG. 14. Simulated heating rates (°C 10^{-4} s^{-1}) at 1200 GMT 21 May 1977: (a) convective and (b) non-convective. The heating rate contour interval is 2. The dashed lines are contours of moist static energy (10^3 m^2 s^{-2}). The moist static energy interval is 10.

ney (1978) found that each of the four models they compared lost energy during the simulation period and it is expected that this model would behave similarly. Note that the KE was generally higher at all levels for the wet simulation than for the dry case, especially in the lower layer. This larger KE of the wet simulation in the lower atmosphere was mainly due to the formation of the low-level jet as shown in the cross sections (Fig. 13). Also, the APE was always lower for the wet case than for the dry case. These two observations suggest that the latent heat aided in the conversion of APE to KE. This agrees with the accepted notion that tropical systems, which are dominated by convection, as was this case, generate KE from vertical transports and energy conversion rather than from the large-scale baroclinic structure which dominates the energy conversions of extratropical systems (Palmén and Newton, 1969). The heating forced the lifting of warmer air and, in return, this upward motion resulted in more latent heat release. This process resulted in a height fall in the lower troposphere and a height increase in the upper troposphere, and thus in the generation of kinetic energy through the ageostrophic component of the wind (Pearce, 1974).

TABLE 1. Computed domain-averaged available potential (APE) and kinetic (KE) energy for the dry simulation. The units are 10^5 J m^{-2}.

Layer (mb)	Energy type	Simulation time (hours) 0	6	12	18	24
850–500	KE	1.77	1.67	1.43	1.35	1.35
500–150	KE	8.79	7.26	7.22	6.80	6.22
850–150	APE	7.66	8.73	8.11	7.12	6.98
	KE	10.56	8.93	8.65	8.15	7.57

6. Summary and conclusions

The effects of latent heating on the development of a wave cyclone and on the large-scale thermodynamics have been investigated using a multi-level primitive equation model. The real-data fine-mesh (~140 km) forecasts, one without latent heating and the other with latent heating, have been carried out for a 24 h period. The former failed to properly predict either the formation of the closed circulation throughout the depth of the troposphere, or the strength of the northwest-to-southeast tilt of the upper-level trough as shown by observations. The latter successfully resolved the abovementioned features and produced very realistic results in the location, intensity and patterns of the observed weather system. The mechanisms for the generation of the regional-scale closed system were examined. Also, the influence of latent heating on the large-scale dynamics and energetics were discussed. These discussions of latent heat effects have focused directly on temperature and thickness fields and associated changes in the wind fields. Of course, the vorticity and vorticity advection fields change accordingly and the

TABLE 2. Computed domain-averaged available potential (APE) and kinetic (KE) energy for the wet simulation. The wet-dry differences are shown in parentheses below their corresponding wet value. The units are 10^5 J m^{-2}.

Layer (mb)	Energy type	Simulation time (hours) 0	6	12	18	24
850–500	KE	1.77	1.66	1.51	1.61	1.57
		(0.00)	(−0.01)	(+0.08)	(+0.26)	(+0.22)
500–150	KE	8.79	7.19	7.18	6.77	6.28
		(0.00)	(−0.07)	(−0.04)	(−0.03)	(+0.06)
	APE	7.66	8.37	7.35	6.34	5.94
		(0.00)	(−0.36)	(−0.76)	(−0.78)	(−1.04)
850–150	KE	10.56	8.85	8.69	8.38	7.85
		(0.00)	(−0.08)	(+0.04)	(+0.23)	(+0.28)

impact of latent heating could have been viewed in these terms as well.

The major findings concluded from the qualitative comparison of these two simulations were that latent heating 1) stabilized the troposphere and reduced the large-scale temperature gradient; 2) decreased the intensity of the large-scale circulation; 3) provided energy for the intensification of the regional-scale closed circulation; and 4) changed the orientation of the large-scale trough and, hence, affected the north-south momentum exchange.

The influence of latent heating on the development of this baroclinically inactive wave cyclone has been explained qualitatively on physical grounds. However, the conclusions should and can be quantified in future studies.

Acknowledgments. The authors wish to thank Ms. Nadine Perkey for her support in preparing the computer forecasts used in this paper. They also wish to thank Dr. Robert Maddox (NOAA-ERL) for his constructive criticism of early drafts of this paper. This work was accomplished as part of the joint project between Drexel University's Atmospheric Sensing and Prediction Project and NCAR's Mesoscale Research Section. This work was performed under Air Force Research Grant F49620-79-C-0208. Also computer time was made available through the Computing Division of the National Center for Atmospheric Research which is sponsored by the National Science Foundation.

REFERENCES

Aubert, E. J., 1957: On the release of latent heat as a factor in large-scale atmospheric motions. *J. Meteor.*, **14,** 527–542.

Bleck, R., 1975: An economical approach to the use of wind data in the optimum interpolation of geo- and Montgomery potential fields. *Mon. Wea. Rev.*, **104,** 807–816.

Baumhefner, D., and P. Downey, 1978: Forecast intercomparisons from three numerical weather prediction models. *Mon. Wea. Rev.*, **106,** 1245–1279.

Chang, C. B., D. J. Perkey and C. W. Kreitzberg, 1981: A numerical case study of the squall line of 6 May 1975. *J. Atmos. Sci.*, **38,** 1601–1615.

Charney, J. G., and A. Eliassen, 1964: On the growth of the hurricane depression. *J. Atmos. Sci.*, **21,** 68–75.

Danard, M. B., 1964: On the influence of released latent heat on cyclone development. *J. Appl. Meteor.*, **3,** 27–37.

Holton, J. R., 1972: *An Introduction to Dynamic Meteorology.* Academic Press, 319 pp.

Kreitzberg, C. W., 1977: SESAME '77 experiments and data availability. *Bull. Amer. Meteor. Soc.*, **58,** 1299–1301.

——, and D. J. Perkey, 1976: Release of potential instability: Part I: A sequential plume model within a hydrostatic primitive equation model. *J. Atmos. Sci.*, **33,** 456–475.

Krishnamurti, T. N., 1968: A study of a developing wave cyclone. *Mon. Wea. Rev.*, **96,** 208–217.

Lorenz, E. N., 1967: *The Nature and Theory of the General Circulation of the Atmosphere.* World Meteorological Organization, No. 218.TP.115, 161 pp.

Palmén, E., and C. W. Newton, 1969: *Atmospheric Circulation Systems.* Academic Press, 603 pp.

Pearce, R. P., 1974: The design and interpretation of diagnostic studies of synoptic-scale atmospheric systems. *Quart. J. Roy. Meteor. Soc.*, **100,** 265–285.

Perkey, D. J., 1976: A description and preliminary results from a fine-mesh model for forecasting quantitative precipitation. *Mon. Wea. Rev.*, **104,** 1513–1526.

——, and C. W. Kreitzberg, 1976: A time-dependent lateral boundary scheme for limited-area primitive equation models. *Mon. Wea. Rev.*, **104,** 744–755.

Tracton, M. S., 1973: The role of cumulus convection in the development of extratropical cyclones. *Mon. Wea. Rev.*, **101,** 573–593.